

AHRS Calibration for a Drill String Sensor Network Application

E. Odei-Lartey, K. A. Hartmann

Zentrum für Sensorsysteme (ZESS),
Universität Siegen, D-57076
Siegen, Germany

email: (elartey,hartmann)@zess.uni-siegen.de

H. Roth

Regelungs- und Steuerungstechnik, Fakultät IV,
Universität Siegen, D-57076
Siegen, Germany

email: hubert.roth@uni-siegen.de

Abstract— In this paper, we illustrate a practical way to determine the systematic error of a micro-electro-mechanical systems inertia measurement unit sensor-based altitude and height reference system mounted on a drill-head for underground navigation. This enables for calibration purposes and for alignment of the system in a designated global reference frame. Furthermore, an extension of this is to enable for onboard real-time calibration in the field with direct access to required parameters over a designed underground wireless ad hoc sensor network telemetry system. This contribution is in line with the embedded systems component of the ubiquitous devices and operative systems track of the conference.

Keywords-calibration; deterministic; stochastic; AHRS; MEMS; sensor guided drill process;

I. INTRODUCTION

Recent developments in the field of wellbore drilling has seen the gradual migration towards the concept of digitalization of key aspects of the entire drilling operation [1]. This has therefore seen the move towards the optimization of drilling operations utilizing the so-called modern technology tools so as to gain economic advantage by way of improving the efficiency of the drilling process [1]. There is therefore a push towards sensor-controlled deep drilling process so as to provide suitable sensor data continuously in real-time. This requires a deeper understanding of multimodal sensors/sensor networks and their conditions of use. Therefore, for field test verification, we have realized an appropriate ad-hoc sensor network along the entire drill string. We also describe the necessity for using a suitable calibration process and give an outlook on how we can generate training data in the next steps to provide a deep neural network solution to process the sensor data.

In our Micro-Electro-Mechanical Systems (MEMS)-based Altitude and Height Reference System (AHRS) for bottom hole trajectory tracking, the main concept is to minimize the errors associated with the IMU sensors before the application of a suitable mathematical model in order to obtain an optimal estimation of the orientation and therefore improve the trajectory of the well path. To facilitate this process is our in-house designed and developed underground wireless ad hoc sensor network borehole telemetry system which allows for real-time data exchange

during a drilling operation irrespective of the drill depth. An extension of this will be to enable the calibration process to be done directly on the field while only communicating the required parameters for the process.

In general, the contribution of this paper is to provide a methodology for MEMS sensor positioning and calibration which can be applied (on-field) by making use of a robotic arm-mounted miniature drill-head where different orientations can be simulated thus representing a multi-position platform for effective sensor calibration. Our robotic-arm-mounted IMU-based AHRS drill-head is programmed at preset orientations whose positions are accurately known from the settings on the robotic arm and used in the estimation of the deterministic errors. The known orientation angles are used with the known local gravity vector to establish the resolved known MEMS accelerometer output data from each of the 3 orthogonal axes which is then used in the determination of the calibration parameters.

Sensor system testing and calibration for Inertial Measurement Unit (IMU)-based navigation systems is of critical importance and has significant consequences in terms of cost and performance of the host vehicle. Basically, the testing and calibration techniques employed needs to reflect the type of application and importantly, the environment in which the sensor and systems are to operate [2]-[6]. Testing is done to enable the output signals to be calibrated and to understand the behavior of the device unit in various situations and environment. In other terms, sensors are calibrated by comparing the analogue or digital signals produced by the sensor with the known input motion. So, for instance, from the rate transfer tests, the output signals from a gyroscope can be compared with the accurately known rotation rate and the scale factor deduced. Also, using gravity vector as an accurate standard, the scale-factor of an accelerometer can be defined. Application of error compensation is then utilized to correct the effects of a predictable systematic error. A basic requirement is that an error process can be represented by an equation and modelled mathematically, and that a signal corresponding to the disturbing effect such as temperature or acceleration, is available and can be measured to the required accuracy [4]. The accuracy that may be achieved from the application of compensation techniques is dependent on precisely how the

coefficients in the “error” equations represents the actual sensor errors. The representation can often vary as a function of time, the environment in which the sensor is used and how often it is used. For more demanding applications, it may be necessary to re-calibrate the sensor regularly, to ensure that the compensation routines are as effective as required by the particular application. Usually, the sensor system is mounted on a multi-axis table or on a rig. The unit may be rotated through a series of accurately known angles and positioned in different orientations with respect to the local gravity vector. The dominant sensor errors may then be determined from static measurements of acceleration and turn rate taken in each orientation of the unit.

In Section II of our paper, we provide an overview of the related works on the approach utilized for IMU sensor calibration. Section III then outlines the general equation model representation for the combined form of the deterministic and stochastic model of the IMU sensor output data. In Section IV, we discuss the calibration process and the methodology for determination of the calibration parameters for finding the deterministic errors associated with two mounted inexpensive MEMS IMU sensors used for the wellbore trajectory tracking process. We then discuss an experimental setup for verification of our calibration process. In Section V, we give the conclusion and an overview of ongoing research in view of the adaptation of deep-learning techniques to improve the calibration process.

II. RELATED WORKS

Introduction to topics surrounding AHRS fail to sufficiently describe the error characteristics of the inertial systems. Inertial system design and performance prediction depends on accurate knowledge of sensor level behavior and therefore it is important to be able to understand and analyze the intrinsic noise characteristics of the IMU sensors to develop the necessary stochastic model to be used in the AHRS model. Generally, the IMU sensor errors are composed of the deterministic and stochastic parts. The main deterministic errors are the bias and misalignment errors. The misalignment errors are composed of the scale factor and the non-orthogonal errors of the sensor [3]-[5]. Laboratory calibration procedures are normally employed in the elimination of these deterministic errors. El-Diasty et al. [3] discussed two calibration methodologies used to find the calibration parameters in order to remove the deterministic errors (systematic errors); inertial biases (bias offset), scale factor and non-orthogonality errors. This involves the six-position static test (up and down position for the inertial sensor axes) [3]-[5]. Basically, the non-orthogonality error is as a result of the imperfect mounting of the IMU sensors along the orthogonal axis at the time of manufacturing. However, in most cases, upon the final integration of the IMU sensor in the final application hardware, there is also the need for a re-calibration of the IMU sensor output as a result of imperfection in the alignment of the IMU sensor

with respect to the final application hardware, which in this case is the drill-head. In the field, there is the difficulty or lack of adequate means to properly re-calibrate the inertial sensors after physically mounting of the hardware on the respective device. This approach therefore provides a means to utilize the drill tube holder which has the ability to be oriented at different angular positions like that of a robotic arm to be utilized for the purposes of calibration.

El-Diasty et al. [3] work is based on the premise that the IMU sensor is in alignment with local gravity vector and therefore gives a general description of how the calibration parameters are determined using the two-position static tests in the zenith direction for the case of the MEMS accelerometer. In their approach, the calibration was done by inducing an excitation signal as input to MEMS accelerometer which is done with local gravity as the excitation/reference signal [3]. In the case of the MEMS gyroscope, the test is done by the use of a two-position dynamic test in any direction [4]. This involves a gyro excitation signal input in the form of a known rotation rate using a calibration turn-table. They discuss further the so-called six position direct method and the six-position weighted least square method approach to determine the inertial bias, scale factor and non-orthogonal deterministic errors. However, for certain applications, this zenith position is determined by the geometry (physical structure) of the application hardware of interest which for our case would be the bottom hole assembly or the drill-head. The sensor reference frame is defined by the body to which the IMU MEMS sensor is strapped unto. This therefore necessitates the need to determine the alignment of the IMU MEMS sensor relative to the body frame of bottom hole assembly or drill-head on which it is mounted. So basically, the final deployment would require for a re-alignment of the IMU MEMS sensors with respect to the drill-head orientation.

III. GENERAL MODEL OF THE IMU SENSOR

The output from the IMU MEMS accelerometer and gyroscope illustrating both the deterministic and stochastic errors is given as shown in (1) and (2). For the MEMS gyroscope triad with instantaneous output $\underline{\omega}_m$, we have

$$\underline{\omega}_m = (\mathbf{M}_g + \delta\mathbf{M}_g) \cdot \underline{\omega} + \underline{b}_g + \delta\underline{b}_g + \underline{w}_g \quad (1)$$

and for the MEMS accelerometer triad with instantaneous linear acceleration output \underline{f}_m , we have

$$\underline{f}_m = (\mathbf{M}_a + \delta\mathbf{M}_a) \cdot \underline{\omega} + \underline{b}_a + \delta\underline{b}_a + \underline{w}_a \quad (2)$$

where $\underline{\omega}$ is the true instantaneous output of the gyroscope triad and \mathbf{M}_a and \mathbf{M}_g represent the 3x3 matrices of the misalignment (scale factor and non-orthogonal) errors of the accelerometer and gyroscope respectively. \underline{b}_a and \underline{b}_g are

the biases in m/s^2 and deg/s respectively for the accelerometer and gyroscope respectively. $\delta\mathbf{M}_a$ and $\delta\mathbf{M}_g$ are 3×3 matrices comprising of the residual scale and non-orthogonal errors (non-diagonal elements), $\delta\mathbf{b}_a$ and $\delta\mathbf{b}_g$ are residual biases, \mathbf{w}_a and \mathbf{w}_g are the zero mean white noise (deg/s for gyros and m/s^2 for acceleration).

So basically the deterministic part of the scale factor and non-orthogonality and the bias can be determined in the laboratory calibration approach that allows for the direct estimation of the bias and misalignment which can be removed from the raw measurements say ω_m and f_m [3]; the raw gyroscope and accelerometer output, before being used in the implementation of the inertial machining equations. The corrected measurements in body reference frame is given as

$$\underline{\omega}_{ib}^b = \delta\mathbf{M}_g \cdot \underline{\omega} + \delta\mathbf{b}_g + \mathbf{w}_g \quad (3)$$

$$\underline{f}^b = \delta\mathbf{M}_a \cdot \underline{f} + \delta\mathbf{b}_a + \mathbf{w}_a \quad (4)$$

Basically $\underline{\omega}_{ib}^b$ and \underline{f}^b still contain random errors: $\delta\mathbf{M}_g$ and $\delta\mathbf{M}_a$ matrices comprising residual scale errors (diagonal elements) and residual non-orthogonal errors (non-diagonal elements) for gyro and accelerometer respectively. El-Diasty et al. [3] also elaborates on the different stochastic models as random constant, random walk, Gauss-Markov process that is used with the Kalman filter for optimal estimation of the gyroscope and accelerometer outputs to provide accurate and continuous navigation solution.

IV. CALIBRATION IN THE GLOBAL REFERENCE FRAME FOR DETERMINISTIC ERRORS

The calibration of our IMU-based AHRS miniature drill-head involved finding the parameters/coefficients that map the measured MEMS accelerometer and gyroscope triad outputs from each sensor's reference frame unto our designated navigation reference frame shown as the global reference frame in Figure 1.

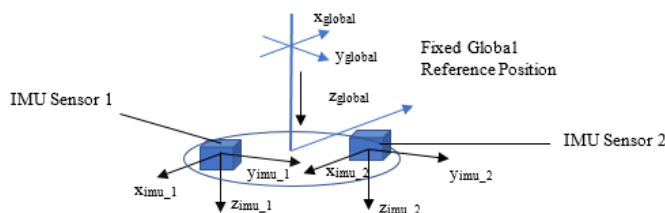


Figure 1a. IMU MEMS sensors mounted on the drill-head and to be aligned to the common global reference frame



Figure 1b. Sensors mounted on the miniature drill-head and further mounted on the KUKA robotic arm

In our setup, for the IMU sensors, we used the Vectornav-100T and the MPU-9255 MEMS sensors which are of industrial and consumer grade respectively. The IMU MEMS accelerometer output data model is represented by the linear equation given as

$$\underline{f}_m = \mathbf{M}_a \cdot \underline{f}_g + \mathbf{b}_a + \mathbf{w}_a \quad (5)$$

where \underline{f}_m is the observed measurement acceleration vector consisting of the outputs of the x, y and z axes of the MEMS accelerometer triad IMU sensor, \underline{f}_g is the resolved accelerometer vector at a preset orientation, \mathbf{M} is the misalignment matrix with the unknown parameters, \mathbf{b} represents the static bias and \mathbf{w} denotes the zero-mean white Gaussian noise. The equation represents that for which a linear regression analysis by which an attempt to find the best, in the least-square sense, straight line to fit a given set of data can be made.

A. Experimental setup and description

Our experimental setup consisted of the two IMU sensors mentioned earlier; Vectornav-100T and the MPU-9255, each composed of a MEMS gyroscope accelerometer triad with axis orthogonal and mounted on a miniature drill-head to form our AHRS integrated system. Eight preset orientations at predefined and accurately measured angles on the Kuka Robot was programmed. At each defined orientation, 1000 measurements were recorded from both sensors at a data rate of 20Hz. This was then used in the formulation given in (6) to generate the unknown regression parameters for the misalignment and bias which minimizes the errors using the maximum likelihood estimation method. Given a set of parameter values with the matrix representation and observations, the estimated regression parameters were determined. The general equation is written in the form.

$$\underline{Y} = \Pi \cdot \underline{\Theta} + \underline{\delta r} \quad (6)$$

This is represented as

$$\underline{Y}_i = \begin{bmatrix} f_{mx_i} \\ f_{my_i} \\ f_{mz_i} \end{bmatrix} \quad (7)$$

$$\Pi_i = \begin{bmatrix} 1 & 0 & 0 & f_{a_{-x_i}} & f_{a_{-y_i}} & f_{a_{-z_i}} & 0 & 0 & 0 & 0 & 0 & 0 \\ 0 & 1 & 0 & 0 & 0 & 0 & f_{a_{-x_i}} & f_{a_{-y_i}} & f_{a_{-z_i}} & 0 & 0 & 0 \\ 0 & 0 & 1 & 0 & 0 & 0 & 0 & 0 & 0 & f_{a_{-x_i}} & f_{a_{-y_i}} & f_{a_{-z_i}} \end{bmatrix} \quad (8)$$

$$\underline{\Theta} = [b_x \ b_y \ b_z \ M_{xx} \ M_{yy} \ M_{zz} \ M_{xy} \ M_{yx} \ M_{yz} \ M_{zy} \ M_{xz} \ M_{zx}]^T \quad (9)$$

$$\underline{\delta r}_i = [w_x \ w_y \ w_z]^T \quad (10)$$

$$\hat{\underline{\Theta}} = (\Pi^T \cdot R^{-1} \cdot \Pi)^{-1} \Pi^T \cdot R^{-1} \cdot \underline{Y} \quad (11)$$

where $\underline{\delta r}$ is the zero-mean white Gaussian noise vector and R is the noise covariance matrix, f_{mx_i} is the x component of the i^{th} measured acceleration. The converted output in the global reference frame is given as

$$\underline{f}_{-g} = M^{-1} \cdot (\underline{f}_{-m} - \underline{b}) \quad (12)$$

Considering the calibration of our drill-head mounted MEMS IMU sensors after mounting both on the robotic arm, as mentioned earlier, the robotic arm was preset to assume a number of orientations to enable the sensor data in the respective orientations to be recorded and used for the calibration process. The calibration entailed the determination of the mapping misalignment matrix and bias vector for the transformation of the sensor output from the sensor reference frame to our designated global/navigation reference frame. In our case, the recordings were done twice in each preset orientation position as observed in Table 1.

TABLE I. CALCULATED X,Y,Z VALUES FOR THE TRUE ACCELERATION VALUES IN A GIVEN ORIENTATION

		h_p	p_1	p_2	p_3	p_4	p_5	p_6	p_7	p_8
Axis	Pitch:	0°	-10°	10°	0°	0°	-10°	10°	0°	0°
	Roll:	0°	0°	0°	-10°	10°	0°	0°	-10°	10°
x	Cal.	0	-0.18	0.18	0.00	0.00	-0.18	0.18	0.00	0.000
y		0	0.00	0.00	-0.18	0.18	0.00	0.00	-0.18	0.176
z		1	0.99	0.99	0.99	0.99	0.99	0.99	0.99	0.985

Table I shows the true accelerometer output approximated to three decimals places for the different orientation

positions (p) preset on the robotic arm with respect to our designated global/navigation reference frame. The recorded measurement in the respective orientation from both MEMS IMU accelerometer sensors is given in Table II. At each orientation position, up to 1000 readings were taken and then afterwards averaged to obtain the respective output on each axis. The output from the Vectornav-100T accelerometer is labelled as the vn_ax, vn_ay and vn_az for the respective x, y, and z axes while for that of the MPU-9255 accelerometer is labelled as mpu_ax, mpu_ay and mpu_az respectively.

TABLE II. ACTUAL ACCELEROMETER OUTPUT IN THE CORRESPONDING ORIENTATION

	vn_ax	vn_ay	vn_az	mpu_ax	mpu_ay	mpu_az
hm_pos	-0.245	0.109	10.276	-0.004	-0.003	1.010
pos_1	0.400	1.681	10.131	0.129	-0.115	0.996
pos_2	-0.883	-1.466	10.123	-0.137	0.110	0.997
pos_3	-1.811	0.749	10.081	0.108	0.129	0.995
pos_4	1.333	-0.533	10.175	-0.116	-0.136	1.000
pos_5	0.368	1.709	10.126	0.132	-0.113	0.996
pos_6	-0.916	-1.436	10.124	-0.133	0.112	0.996
pos_7	-1.848	0.778	10.070	0.111	0.132	0.993
pos_8	1.296	-0.505	10.179	-0.113	-0.133	1.000

The recorded MEMS accelerometer triads output data shown in Table 2 were then used as the observation representation in equation (6) and the maximum likelihood method was used to determine the systematic mapping bias vector and scale factor and non-orthogonal mapping matrix that is used for the transformation from each sensor's reference frame to our designated global/navigation reference frame.

The results for the generated Vectornav-100T misalignment and bias were found to be:

$$M_{VN_a} = \begin{pmatrix} -3.820 & 8.100 & -1.465 \\ -9.005 & -3.826 & 0.966 \\ -0.012 & 0.293 & 9.625 \end{pmatrix}$$

$$\underline{b}_{VN_a} = \begin{pmatrix} 1.188 \\ -0.822 \\ 0.644 \end{pmatrix} \quad (13)$$

The generated MPU-9255 accelerometer misalignment and bias was determined to be:

$$M_{MPU9255_a} = \begin{pmatrix} -0.754 & -0.658 & 0.082 \\ 0.658 & -0.753 & 0.010 \\ 0.001 & 0.016 & 1.061 \end{pmatrix}$$

$$\underline{b}_{MPU9255_a} = \begin{pmatrix} -0.076 \\ -0.093 \\ -0.052 \end{pmatrix} \quad (14)$$

Conceptually, an unlimited or arbitrary number of different preset locations can be utilized for generating the true outputs to be used in the bias vector and misalignment vector determination process. However, the number of observations/measurements should be equal or greater than the number of unknown parameters to ensure a non-underdetermined system.

For the determination of the calibration parameters of the MEMS IMU gyroscope triad, the high resolution, high accurate calibration turn-table was utilized. With rotation in the clockwise direction considered positive, two preset rotation speeds of equal magnitudes at 200 degrees per second ($^{\circ}/s$) but in opposite directions were applied to each axis while the axis of interest was aligned with gravity in the upwards direction on the turn table as shown in Figure 4.

TABLE III. THE PRESET RATE OF 200 $^{\circ}/s$ APPLIED BOTH CLOCKWISE (C.W.) AND ANTI-CLOCKWISE (A-C.W.) TO THE TURN TABLE WITH EACH AXIS IN TURN ALIGNED WITH GRAVITY IN THE UPWARDS DIRECTION

axis	rate	x c.w. ($^{\circ}/s$)	x a-c.w. ($^{\circ}/s$)	y c.w. ($^{\circ}/s$)	y a-c.w. ($^{\circ}/s$)	z c.w. ($^{\circ}/s$)	z a-c.w. ($^{\circ}/s$)
x	200 $^{\circ}/s$	200.00	-200.00	0.00	0.00	0.00	0.00
y	200 $^{\circ}/s$	0.00	0.00	200.00	-200.00	0.00	0.00
z	200 $^{\circ}/s$	0.00	0.00	0.00	0.00	200.00	-200.00

Again 1000 readings were taken and then afterwards averaged to obtain the respective output on each axis as shown in Table 4. The results of the readings from Table IV were then used as the observations representation in equation (6) and the maximum likelihood method again used for the determination of the misalignment and bias mapping matrix and vector respectively. Temperature dependency was considered such that the misalignment and the bias were recalculated according to the corresponding sensitivities per degree increase in temperature of both MEMS IMU accelerometer and gyroscope triads.

TABLE IV. RECORDED VECTOR-100T GYROSCOPE OUTPUT IN THE RESPECTIVE POSITIONS

axis	x c.w. ($^{\circ}/s$)	x a-c.w. ($^{\circ}/s$)	y c.w. ($^{\circ}/s$)	y a-c.w. ($^{\circ}/s$)	z c.w. ($^{\circ}/s$)	z a-c.w. ($^{\circ}/s$)
x	-185.875	185.741	74.060	-74.429	0.068	-0.353
y	-72.021	71.948	-186.627	186.225	0.156	0.418
z	-2.667	2.601	0.633	-1.004	199.412	-199.75

The generated Vectornav-100T gyroscope misalignment and bias was determined to be:

$$M_{VN_g} = \begin{pmatrix} -0.929 & -0.360 & -0.013 \\ 0.371 & -0.932 & 0.004 \\ 0.001 & -0.001 & 0.998 \end{pmatrix}$$

$$\underline{b}_{VN_g} = \begin{pmatrix} -0.046 \\ -0.190 \\ -0.008 \end{pmatrix} \quad (15)$$

TABLE V. RECORDED MPU-9255 GYROSCOPE OUTPUT IN THE RESPECTIVE POSITIONS

axis	x c.w. ($^{\circ}/s$)	x a-c.w. ($^{\circ}/s$)	y c.w. ($^{\circ}/s$)	y a-c.w. ($^{\circ}/s$)	z c.w. ($^{\circ}/s$)	z a-c.w. ($^{\circ}/s$)
x	127.8232	-127.678	154.0631	-154.038	2.809	-2.849
y	-154.261	154.480	126.568	-126.565	0.930	-1.047
z	-0.976	1.120	-0.001	-0.013	200.138	-200.338

The generated MPU-9255 gyroscope misalignment and bias was determined to be:

$$M_{MPU9255_g} = \begin{pmatrix} 0.639 & -0.772 & -0.005 \\ 0.770 & 0.633 & 0.000 \\ -0.014 & 0.005 & 1.001 \end{pmatrix}$$

$$\underline{b}_{MPU9255_g} = \begin{pmatrix} 0.085 \\ 0.002 \\ -0.059 \end{pmatrix} \quad (16)$$

B. Verification of Calibration

For the verification of our calibration process, the Kuka robotic arm was then programmed for motion along a specified trajectory. The trajectory involved the movement of the drill head from a station position A, through station position B and finally settling at position point C. In this setup the vertical displacement from A to B was made with a distance of 0.5m. The position C was then set at an inclination angle of about 30 $^{\circ}$ from station position B and also with a displacement of 0.5m from B. We then established the ground truth of our drill-head trajectory based on the Kuka robots coordinate system with the points A, B and C as shown in Figure 2. The points of the station positions A, B and C were referenced to a central reference point on the robot. To determine the true geometric measurements, the numerical values of the positions given as vector coordinates indicated by the robotic PLC read out was used. Note that the measurements were given in millimeters. For actual verification of the trajectory of the miniature drill-head, a recording of the changing position vector coordinates was made and graphed to give a good representation of the ground truth from the perspective of

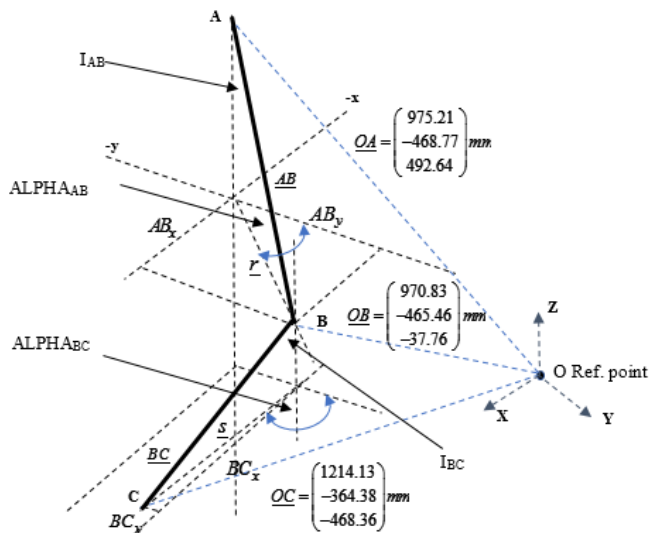


Figure 2. The geometric diagram showing the vector coordinates of the station positions A, B, and C on the Kuka Robot and from which the true trajectory of the drill-head is determined

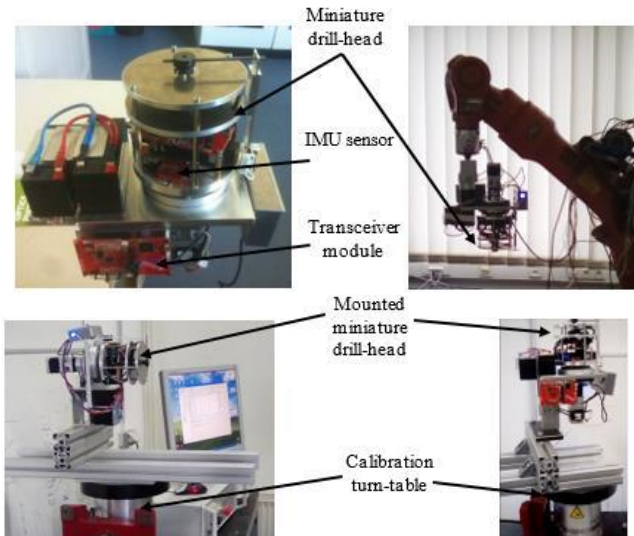


Figure 3. Top left is the miniature drill-head (AHRS) with the mounted IMU sensors and a wireless transceiver module for data acquisition. Top right is it mounted on the robotic arm. Bottom is the calibration turn-table with it mounted for calibration of the MEMS gyroscope triad.

the robotic arm. Only the trajectory and drill-head orientation were of interest. In Figure 3, the mounting positions of the miniature drill-drill head on the robotic arm as well as the turn-table for the static measurements are shown. From the station position vector coordinates, A, B, C, the distance traversed from station A through station B to station C is determined from the readout of the robot coordinate system. From the Figure 2 information, we can easily compute the respective displacement vectors and consequently the distance from position A to position B. Figures 4-7 show the output of the two MEMS accelerometer and gyroscope triads; MPU-9255 and vectornav-100T, during translational motion in both the

body frame of reference and the designated global/navigation reference frame. The two IMU sensors were mounted on different positions on the drill-head setup. Figure 4 shows the respective 3-axis accelerometer output which reflects difference in mounting positions. After application of the determined bias vector and misalignment matrices, the resulting converted outputs of the respective MEMS accelerometer and gyroscope triads in the global reference frame were plotted as shown in Figure 6. The outputs of both sensors show the expected similarity in values after the removal of the deterministic bias offset, scale factor and non-orthogonal systematic errors.

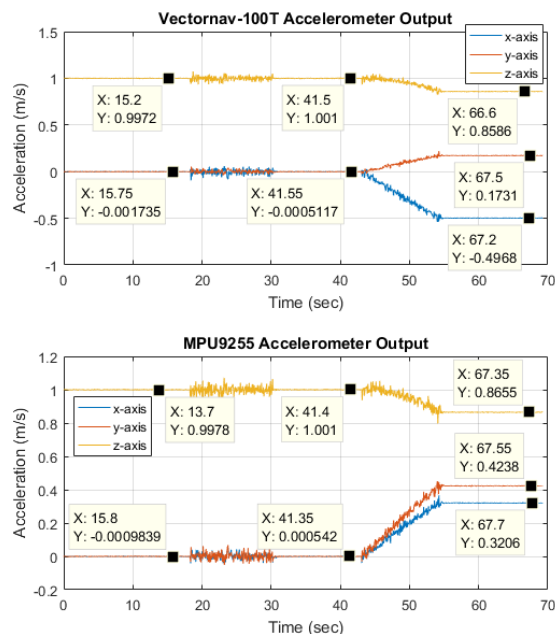


Figure 4. Measured IMU accelerometer output BEFORE conversion to global reference

This converted output data, after denoising, is then used as the input source in the AHRS model for the respective orientation estimation and consequently the overall the wellbore trajectory determination. Slight differences in output can be explained as the effects of temperature variations within the laboratory environment. The random errors left afterwards are the residual bias and residual misalignment errors which could then be stochastically modelled and utilized in the optimal estimator for the trajectory tracking process.

Improvement of the overall accuracy of the measurement can also be attributed to both the number and performance specification of the individual sensors used within a cluster or single node which is calibrated.

V. CONCLUSION, ONGOING RESEARCH AND OUTLOOK

The aim is to enable an adoptable concept of the algorithm to be directly implementable on the onboard microprocessor

with the required parameters transferred to all sensor node modules over the underground wireless ad hoc network to facilitate the calibration process in real-time. Taking into consideration recent trends in machine learning and neural networks [11], a possible extension of this calibration process is with the use of multiple point measurements with the respective output data as training data within a neural network. Investigation into the possibility of improving the estimation of well-bore trajectory tracking utilizing the concept of artificial neural networks for predicting the orientation of the drill-head or bottom hole assembly would be of great interest.

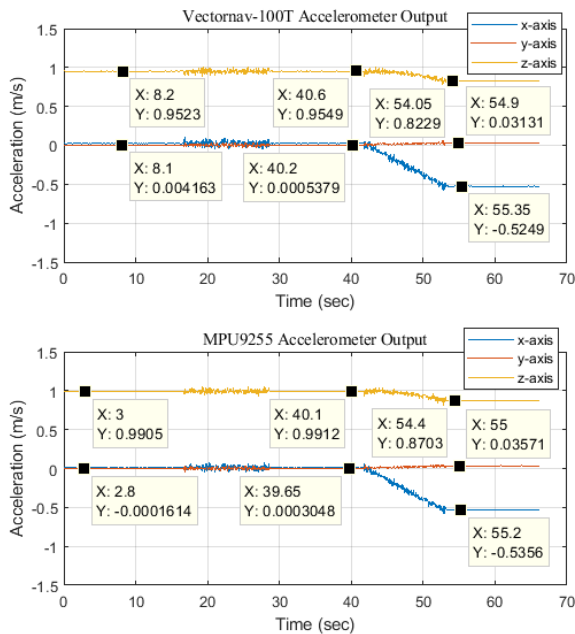


Figure 5. Measured IMU accelerometer output AFTER conversion to global reference

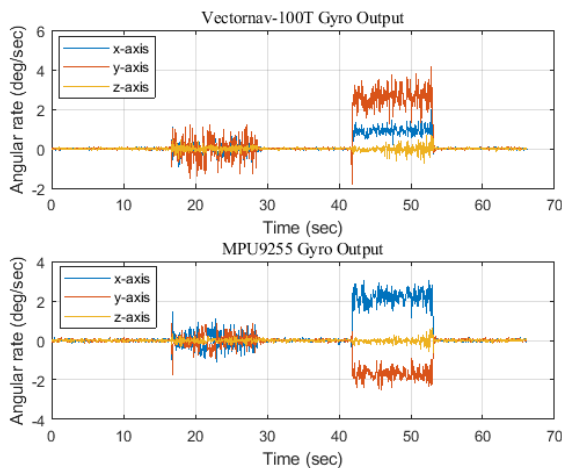


Figure 6. Measured IMU gyroscope output BEFORE conversion to global reference

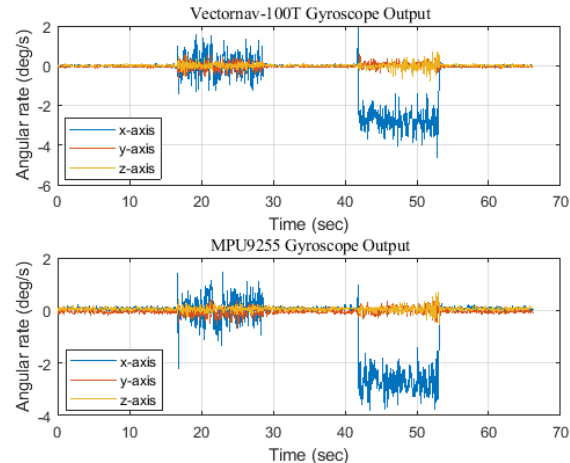


Figure 7. Measured IMU gyroscope output AFTER conversion to global reference

This notwithstanding, will not completely discard the current concept of using appropriate navigation models, such as the AHRS mathematical model in conjunction with an optimal estimator for continuously tracking the drill-head/bottom hole assembly, but would rather serve to complement the other. The concept for a laboratory setup is to use the miniature drill-head-mounted on the robotic arm to generate training data to be used in determining the different orientations of the drill-head during underground borehole navigation. The aim is to generate a proper set of coordinates characterizing a set of landmarks as inputs from the relevant sensors and the outputs characterizing the correlating orientation positions or the transformed orientation position. Theoretically, there will be an infinity of positions in the input landmark set or data points which will capture all possible orientations of the drill head relative to a designated frame of reference. In practicality, a couple of important beacon positions with their corresponding output landmarks set could be carefully selected and used as training data. This can then be extrapolated to capture all possible representations of the orientation. Controlled temperature (and pressure condition) could be included in the training data set to capture the effect of temperature rise on the IMU sensor data output.

The machination equation will be used in the optimal estimator filter in the classical sense for estimation of the bottom hole assembly/drill head orientation and the output fused or used as extra information in addition to the output generated by the artificial neural network. This technique would serve as an extension to find a more accurate estimate of the overall well-bore trajectory estimation. A comparison of the results of the optimal filter to that of the artificial neural network could be evaluated and further used as training data set to improve the neural network.

ACKNOWLEDGMENT

Thanks goes to Peter Sahn of the RST robotic laboratory, Faculty IV, Universität Siegen for his assistance in the KUKA robotic arm setup and programming to enable

for the measurements to be taken. Also, thanks to Bodo Ohrndorf and Peter Hof for their technical assistance in the miniature drill-head and turn-table setup.

REFERENCES

- [1] "The digital oilfield" Drilling Contractor, International Association of Drilling Contractors (IADC), Vol. 75, No. 4, July/August 2019
- [2] P. Maybeck, "Stochastic Models, Estimation and Control: Volume 1", Department of Electrical Engineering, Air Force Institute of Technology, Wright-Patterson Air Force Base, Ohio, Academic Press, New York, Inc.
- [3] M. El-Diasty and S. Pagiatakis, "Calibration and Stochastic Modelling of Inertial Navigation Sensor Errors", Dept. of Earth & Space Science & Engineering, York University, Journal of Global Positioning Systems, Vol.7. No. 2: 170-182, pp. 170-182, 12/2008.
- [4] H. Titterton and J.L. Weston, "Strapdown Inertial Navigation Technology – 2nd Edition," The Institute of Electrical Engineering and Technology, London, United Kingdom and The American Institute of Aeronautics, Reston, Virginia, USA, 2004.
- [5] A. Quinchia and G. Falco, E. Falletti, F. DAVIS, C. Ferrer, "A Comparison between Different Error Modeling of MEMS Applied to GPS/INS Integrated Systems", Open Access, Sensors, ISSN 1424-8220, July 2013.
- [6] IEEE Standard Specification Format Guide and Test Procedure for Single-Axis Interferometric Fiber Optic Gyros; IEEE Std 952-1997; IEEE: New York, NY, USA, 1998.
- [7] A. G. Quinchia, G. Falco, E. Falletti, F. DAVIS, and C. Ferrer, "A Comparison between Different Error Modeling of MEMS Applied to GPS/INS Integrated Systems," Open Access, Sensors ISSN 1424-8220, p. 9549, 08/2013.
- [8] N. El-Sheimy, H. Hou, and X. Niu, "Analysis and Modeling of Inertial Sensors Using Allan Variance," IEEE Transactions on Instrumentation and Measurement, Vol. 57. No. 1, pp. 140-149, January 2008.
- [9] A. Radi, S. Nassar, and N. El-Sheimy, "Stochastic Error Modeling of Smartphone Inertial Sensors for Navigation in Varying Dynamic Conditions", ISSN 2075-1087, Gyroscopy and Navigation, Vol. 9, No. 1, pp. 76-95, 2018.
- [10] O. Woodman, "An introduction to inertial navigation" Technical Report, University of Cambridge Computer Laboratory Number 696, United Kingdom, ISSN 1476-2986, 2007.
- [11] B. Zhang, I. Horvath, and J. Molenbroek, C. Snijders, "Using artificial neural networks for human body posture prediction", International Journal of Industrial Ergonomics, ScienceDirect, Elsevier, 2010.